AD-A215 476

(2)

REPORT DOCUMENTATION PAGE

Form Approved
OMB No. 0704-0188

1. AGENCY USE ONLY (Leave blank)	2. REPORT DATE	3. REPORT TYPE AND DATES COVERED
	April 1982	Final (1 Jun 81-31 Mar 82

4. TITLE AND SUBTITLE

THE ROOM-TEMPERATURE SHAPES OF FOUR-LAYER UNSYMMETRIC CROSS-PLY LAMINATES

5. FUNDING NUMBERS

61102F

2307/D9

6. AUTHOR(S)

Michael W. Hyer

7. PERFORMING ORGANIZATION NAME(S) AND ADDRESS(ES)

Virginia Polytechnic Inst & State University
Dept of Engineering Science and Mechanics
Blacksburg, VA 24061-4899

8. PERFORMING ORGANIZATION REPORT NUMBER

VPI-E-82-15

9. SPONSORING/MONITORING AGENCY NAME(S) AND ADDRESS(ES)

AFOSR
BLDG 410
BAFB DC 20332-6448

10. SPONSORING/MONITORING AGENCY REPORT NUMBER

AFOSR-81-0195

11. SUPPLEMENTARY NOTES

12a. DISTRIBUTION/AVAILABILITY STATEMENT

DISTRIBUTION STATEMENT A
Approved for public release;
Distribution Unlimited

12b. DISTRIBUTION CODE

13. ABSTRACT (Maximum 200 words)

14. SUBJECT TERMS

15. NUMBER OF PAGES
48

16. PRICE CODE

17. SECURITY CLASSIFICATION OF REPORT	18. SECURITY CLASSIFICATION OF THIS PAGE	19. SECURITY CLASSIFICATION OF ABSTRACT	20. LIMITATION OF ABSTRACT
unclassified	unclassified		

College of Engineering

Virginia Polytechnic Institute and State University

Blacksburg, VA 24061

VPI-E-82-12 April 1982

The Room-Temperature Shapes of Four-Layer Unsymmetric Cross-Ply Laminates

Michael W. Hyer[1]

Prepared for

Dr. Anthony K. Amos
Air Force Office of Scientific Research/NA
Bolling Air Force Base
Washington, DC 20332

under Grant AFOSR-81-0195

(1) Associate Professor, Engineering Science and Mechanics
Virginia Polytechnic Institute and State University
Blacksburg, VA 24061-4899

BIBLIOGRAPHIC DATA SHEET	1. Report No.	2.	3. Recipient's Accession No.

4. Title and Subtitle

The Room-Temperature Shapes of Four-Layer Unsymmetric Cross-Ply Laminates

5. Report Date: April 1982

6.

7. Author(s): Michael W. Hyer

8. Performing Organization Rept. No. VPI-E-82-12

9. Performing Organization Name and Address

Department of Engineering Science and Mechanics
Virginia Polytechnic Institute and State University
Blacksburg, VA 24061-4899

10. Project/Task/Work Unit No.

11. Contract/Grant No.: AFOSR-81-0195

12. Sponsoring Organization Name and Address

Dr. Anthony K. Amos
Air Force Office of Scientific Research/NA
Bolling Air Force Base
Washington, DC 20332

13. Type of Report & Period Covered: Final Report: 6/81-3/82

14.

15. Supplementary Notes

16. Abstracts

A previous approximate theory for predicting the room-temperature shapes of unsymmetric laminates is examined in light of the assumptions regarding the inplane strains. The previous theory, which was a geometrically nonlinear extension of classical lamination theory, was felt to be restrictive and this paper develops a new theory in which these restrictions are relaxed. It is shown that despite the previous concern, there is little difference between the previous theory and this theory. This paper presents numerical results for the inplane residual strains of unsymmetric laminates which have cooled from curing into a cylindrical room-temperature shape. It is shown that the residual strains are compressive and practically independent of spatial location on the laminate. In another facet of the paper, the room-temperature shapes of all four-layer unsymmetric cross-ply laminates are predicted. There are only four unique stacking arrangements for this category of laminates and it is shown that their shapes are a strong function of their size and their stacking arrangement.

17. Key Words and Document Analysis. 17a. Descriptors

composites
structures
plates
shells

17b. Identifiers/Open-Ended Terms

composite materials, unsymmetric laminates, thermal stresses, thermal buckling, residual stresses, cross-ply laminates

17c. COSATI Field Group 39

18. Availability Statement	19. Security Class (This Report) UNCLASSIFIED	21. No. of Pages 43
	20. Security Class (This Page UNCLASSIFIED	22. Price

INSTRUCTIONS FOR COMPLETING FORM NTIS-35 (Bibliographic Data Sheet based on COSATI Guidelines to Format Standards for Scientific and Technical Reports Prepared by or for the Federal Government. PB-180 600).

1. **Report Number.** Each individually bound report shall carry a unique alphanumeric designation selected by the performing organization or provided by the sponsoring organization. Use uppercase letters and Arabic numerals only. Examples FASEB-NS-73-87 and FAA-RD-73-09.

2. Leave blank.

3. **Recipient's Accession Number.** Reserved for use by each report recipient.

4. **Title and Subtitle.** Title should indicate clearly and briefly the subject coverage of the report, subordinate subtitle to the main title. When a report is prepared in more than one volume, repeat the primary title, add volume number and include subtitle for the specific volume.

5. **Report Date.** Each report shall carry a date indicating at least month and year. Indicate the basis on which it was selected (e.g., date of issue, date of approval, date of preparation, date published).

6. **Performing Organization Code.** Leave blank.

7. **Author(s).** Give name(s) in conventional order (e.g., John R. Doe, or J.Robert Doe). List author's affiliation if it differs from the performing organization.

8. **Performing Organization Report Number.** Insert if performing organization wishes to assign this number.

9. **Performing Organization Name and Mailing Address.** Give name, street, city, state, and zip code. List no more than two levels of an organizational hierarchy. Display the name of the organization exactly as it should appear in Government indexes such as Government Reports Index (GRI).

10. **Project/Task/Work Unit Number.** Use the project, task and work unit numbers under which the report was prepared.

11. **Contract/Grant Number.** Insert contract or grant number under which report was prepared.

12. **Sponsoring Agency Name and Mailing Address.** Include zip code. Cite main sponsors.

13. **Type of Report and Period Covered.** State interim, final, etc., and, if applicable, inclusive dates.

14. **Sponsoring Agency Code.** Leave blank.

15. **Supplementary Notes.** Enter information not included elsewhere but useful, such as: Prepared in cooperation with . . . Translation of . . . Presented at conference of . . . To be published in . . . Supersedes . . . Supplements . . . Cite availability of related parts, volumes, phases, etc. with report number.

16. **Abstract.** Include a brief (200 words or less) factual summary of the most significant information contained in the report. If the report contains a significant bibliography or literature survey, mention it here.

17. **Key Words and Document Analysis. (a). Descriptors.** Select from the Thesaurus of Engineering and Scientific Terms the proper authorized terms that identify the major concept of the research and are sufficiently specific and precise to be used as index entries for cataloging.
(b). Identifiers and Open-Ended Terms. Use identifiers for project names, code names, equipment designators, etc. Use open-ended terms written in descriptor form for those subjects for which no descriptor exists.
(c). COSATI Field/Group. Field and Group assignments are to be taken from the 1964 COSATI Subject Category List. Since the majority of documents are multidisciplinary in nature, the primary Field/Group assignment(s) will be the specific discipline, area of human endeavor, or type of physical object. The application(s) will be cross-referenced with secondary Field/Group assignments that will follow the primary posting(s).

18. **Distribution Statement.** Denote public releasability, for example "Release unlimited", or limitation for reasons other than security. Cite any availability to the public, other than NTIS, with address, order number and price, if known.

19 & 20. **Security Classification.** Do not submit classified reports to the National Technical Information Service.

21. **Number of Pages.** Insert the total number of pages, including introductory pages, but excluding distribution list, if any.

22. **NTIS Price.** Leave blank.

Preface

The enclosed report is a copy of a paper submitted for publication consideration in the Journal of Composite Materials. The issuing of the paper in this report format is for the purposes of reporting research findings to the agency which sponsored the work. The issuing of the report is not meant to duplicate the efforts of the Journal of Composite Materials.

Abstract

A previous approximate theory for predicting the room-temperature shapes of unsymmetric laminates is examined in light of the assumptions regarding the inplane strains. The previous theory, which was a geometrically nonlinear extension of classical lamination theory, was felt to be restrictive and this paper develops a new theory in which these restrictions are relaxed. It is shown that despite the previous concern, there is little difference between the previous theory and this theory. This paper presents numerical results for the inplane residual strains of unsymmetric laminates which have cooled from curing into a cylindrical room-temperature shape. It is shown that the residual strains are compressive and practically independent of spatial location on the laminate. In another facet of the paper, the room-temperature shapes of all four-layer unsymmetric cross-ply laminates are predicted. There are only four unique stacking arrangements for this category of laminates and it is shown that their room-temperature shapes are a strong function of their size and their stacking arrangement. Depending on these parameters, the room-temperature shape of a four-layer cross-ply unsymmetric laminate can be a unique saddle shape, a unique cylindrical shape, or a cylindrical shape that can be snapped through to another cylindrical shape.

Introduction

Recently Hyer reported on a series of experiments [1] and a theory [2] aimed at understanding the phenomena which govern the room-temperature shapes of unsymmetrically laminated composites. Specifically, the studies were concerned with $[0_2/90_2]_T$ and $[0_4/90_4]_T$ laminates which are fabricated on a flat plate, cured at an elevated temperature, and allowed to cool to room temperature. The studies were initiated because it had been reported by many investigators that the room-temperature shapes of unsymmetric laminates did not always conform to the predictions of classical lamination theory. Instead of being saddle shaped, as classical lamination theory predicts, the room-temperature shapes of unsymmetrically laminated composites are often cylindrical in nature. In addition, a second cylindrical shape can sometimes be obtained from the first by a simple snap-through action. The experiments quantified some of these effects while the theory was developed to explain the mechanics of the laminates.

By extending classical lamination theory to include geometric nonlinearities, many of the qualitative and quantitative characteristics of unsymmetric laminates were explained. The extended theory was approximate in nature, using assumed displacement functions in conjunction with a Rayleigh-Ritz minimization of the total potential energy. For a given lay-up, the theory predicts $[0_2/90_2]_T$ and $[0_4/90_4]_T$ laminates to have either a single unique shape or one of three possible shapes. The specific shape depends on the size of the laminate. When the sidelength of a square laminate is smaller than a certain critical length, a unique saddle shape is predicted. When the sidelength is larger than this critical value, either a saddle or one of two possible cylindrical

shapes is predicted. The thickness of the laminate also has a bearing on the saddle-cylinder behavior. A stability analysis shows that when three shapes are predicted, the saddle shape corresponds to an unstable equilibrium configuration. Both of the two cylindrical shapes of the triple-valued solution correspond to stable equilibrium configurations. When the saddle shape is the only shape predicted, it is found to be stable. Correlation between the theory and the limited amount of experimental data is good. Recently Hahn [3] and Hahn and Hwang [4] have reported on further experiments designed to check the theory. They studied the effect of sidelength on the shapes of $[0_4/90_4]_T$ laminates and found reasonable agreement between Hyer's theory and their experiments.

While the series of experiments Hyer conducted involved a wide variety of unsymmetric lay-ups, his theory was restricted to the study of $[0_2/90_2]_T$ and $[0_4/90_4]_T$ laminates. This limitation was imposed in order to keep the algebra at a minimum but still retain the basic idea of asymmetry. In arriving at the theoretical predictions, Hyer used simple polynomials to approximate the three components of displacement in the Rayleigh-Ritz scheme. Use of these polynomials led to two coupled nonlinear algebraic equations. These equations were solved numerically and the solution of these equations led directly to the predicted shapes. The polynomials used in the displacement approximations were of a low order so that the number of nonlinear equations would be kept at a minimum. Because of the good correlation between the theory and the available experimental data, the polynomials chosen apparently modeled the shape behavior correctly. The question was raised, however, about the use of more sophisticated polynomials, particularly for approximating

the inplane displacements. The out-of-plane displacements were associated with the shapes and experimental observation led to the form of the approximating functions for these displacements. It was found from the experiments that polynomials were sufficient. However, the in-plane displacements were not as observable and so there was a lack of physical evidence for choosing any particular functional form for those displacements. Polynomials were chosen, as opposed to other functional forms, so that all of the approximating functions would at least be of similar algebraic form and thus ease some of the mathematical and algebraic manipulations. As is well known, when using a classical Rayleigh-Ritz approach, approximating functions must be chosen which are valid over the entire spatial domain. The approximating functions must be chosen to have enough freedom to accurately model complex behavior over the domain. Complex behavior may well not exist but if the possibility is not allowed for in the approximate functional form, complex behavior may be overlooked when it does occur. For elastic systems, such as laminates, not having enough freedom in the approximate displacement functions leads to a system which acts much stiffer than the system it is modeling. Thus, to examine the effects on previous predictions of choosing more sophisticated functions for the approximate inplane displacement fields, and to generate new results for unsymmetric laminates, the analytical work has continued beyond the initial studies. This paper reports on the additional work and shows the effect of including more sophisticated displacement functions. Also, some new and interesting results for unsymmetric laminates are presented.

Specifically, the paper examines the room-temperature shapes of all square unsymmetric cross-ply laminates which can be fabricated from four

layers. There are only four unique unsymmetric laminates in this category, all other laminates being obtainable from these four by simple rotations. The four unique laminates are: $[0/0/0/90]_T$, $[0/0/90/0]_T$, $[0/90/0/90]_T$, and $[0/0/90/90]_T$. The last stacking arrangement was the one examined in the previous paper. In the notation used here, the left-most entry in the stacking sequence nomenclature corresponds to the orientation, relative to the laminate x axis, of the fibers in the lamina at the negative-most z location. As will be seen, $[0/90/0/90]_T$ laminates behave in a manner similar to $[0/0/90/90]_T$ laminates. However, $[0/0/0/90]_T$ and $[0/0/90/0]_T$ laminates behave quite differently. The analytical procedure used in these latest studies parallels the approach in the previous paper. For this reason some of the details of the analysis are omitted. This paper emphasizes the assumptions used in the analyses. The interested reader is encouraged to read the previous work.

Problem Statement

Figure 1 illustrates the problem in question and defines the coordinate system used in the study. Figure 1a illustrates the flat laminate in the uncured state, or in the cured state at the elevated curing temperature. As the laminate cools from the curing temperature, the through-the-thickness lack of symmetries in the thermoelastic properties of the laminate causes it to warp out of plane. The out-of-plane displacements are accompanied by inplane displacements but, as stated before, these are not as evident to an observer. Figure 1b shows the cooled laminate in a saddle shape and figs. 1c and 1d show the laminate in cylindrical shapes. As can be seen in the figure, the curvatures of the saddle are not necessarily equal nor are the curvatures of the two cylinders necessarily equal. This paper investigates the parameters which influence whether the flat laminate of fig. 1a cures and cools to the shape given by fig. 1b, 1c, or 1d. The solution procedure seeks the shape (or shapes) that minimizes the total potential energy of the laminate.

Assumed Displacement Functions

As in the previous work, the approximation to the out-of-plane displacement, w, is chosen to be

$$w(x,y) = \frac{1}{2}(ax^2 + by^2), \tag{1}$$

with a and b to-be-determined constants which dictate the shape of the laminate. The case $a > 0$, $b < 0$ corresponds to the saddle of fig. 1b while the case $a > 0$, $b = 0$ corresponds to the cylinder of fig. 1c. The case $a = 0$, $b < 0$ is another cylinder and is illustrated in fig. 1d. In the earlier work, the inplane displacements of the laminate's midplane in the x and y directions, $u^0(x,y)$ and $v^0(x,y)$ respectively, were approximated using the following logic: Due to the fact that the out-of-plane displacements of unsymmetric laminates are many times the laminate thickness, the von Kármán approximation to Green's strain measures should be used. Accordingly, the strain-displacement relations are

$$e_{11} = \varepsilon_x^0 - z\frac{\partial^2 w}{\partial x^2} \tag{2}$$

$$e_{22} = \varepsilon_y^0 - z\frac{\partial^2 w}{\partial y^2} \tag{3}$$

$$e_{12} = \varepsilon_{xy}^0 - z\frac{\partial^2 w}{\partial y \partial x}, \tag{4}$$

where 1 is associated with the x direction and 2 is associated with the y direction. The inplane strains, ε_x^0, ε_y^0, and ε_{xy}^0, are given by

$$\varepsilon_x^0 = \frac{\partial u^0}{\partial x} + \frac{1}{2}\left(\frac{\partial w}{\partial x}\right)^2 \tag{5}$$

$$\varepsilon_y^0 = \frac{\partial v^0}{\partial y} + \frac{1}{2}\left(\frac{\partial w}{\partial y}\right)^2 \tag{5}$$

$$\varepsilon_{xy}^0 = \frac{1}{2}\left\{\frac{\partial u^0}{\partial y} + \frac{\partial v^0}{\partial x} + \frac{\partial w}{\partial x}\frac{\partial w}{\partial y}\right\} . \tag{7}$$

It was assumed that the vast majority of the u^0 displacement would be due to the curling up of the laminate in the x-z plane. Referring to fig. 2, even though there may not be much strain in line elements originally in the x direction, these line elements undergo large negative displacements in the x direction. When the laminate is flat, the distance to point A, from the origin 0, is x. When the laminate curls into a cylinder of radius ρ with generators perpendicular to the x-z plane, the arc length from 0 to A is still very close to being x. However, point A has moved in the x-direction an amount

$$u^0 = \rho \sin\theta - x , \tag{8}$$

where θ is the angular location, as measured from the vertical z-axis of point x. For cylinders with small angular openings

$$\sin\theta = \theta - \frac{\theta^3}{3!} + \ldots \tag{9}$$

By geometry, assuming the inplane (arc-wise) strains are negligible, the length from 0 to x is given by

$$x = \rho\theta . \tag{10}$$

From eq. 1,

$$\rho \approx \frac{1}{a} . \tag{11}$$

Using eqs. 9, 10, and 11 in eq. 8 leads to an approximate expression for the x-direction displacement at point A due to curling, namely

$$u^0 = - \frac{x^3 a^2}{6} . \tag{12}$$

A similar argument was made for curling in the y-z plane. Thus, the y-direction displacement due to cylindrical curling in the y-z plane was given by

$$v^0(x,y) = - \frac{y^3 b^2}{6} . \tag{13}$$

Continuing to construct u^0 and v^0 on physical grounds, it was further argued that the inplane strains were similar to the predictions of classical lamination theory in that they were independent of x and y. Thus terms were added to eqs. 12 and 13 which led to constant inplane strains ε_x^0 and ε_y^0. These added terms were cx for eq. 12 and dx for eq 13, c and d to-be-determined constants. At this point the inplane strains were of the form

$$\varepsilon_x^0 = c \tag{14}$$

$$\varepsilon_y^0 = d \tag{15}$$

$$\varepsilon_{xy}^0 = \frac{abxy}{2} . \tag{16}$$

As a final step, it was reasoned that for cross-ply laminates there would be no inplane shearing strains. This is the classical lamination theory prediction and it was assumed to be true for this large-deflection problem. Equation 16 contradicted this assumption and so u^0 and v^0 were appended to result in $\varepsilon^0_{xy} = 0$. The final approximate forms for u^0 and v^0 were

$$u^0(x,y) = cx - \frac{a^2 x^3}{6} - \frac{abxy^2}{4} \tag{17}$$

and

$$v^0(x,y) = dy - \frac{b^2 y^3}{6} - \frac{abx^2 y}{4} , \tag{18}$$

where the 3rd term in each equation was added to result in zero inplane shear strain. These equations, along with eq. 1, led directly to the following form for the inplane strains,

$$\varepsilon^0_x = c - \frac{aby^2}{4} , \tag{19}$$

$$\varepsilon^0_y = d - \frac{abx^2}{4} , \tag{20}$$

$$\varepsilon^0_{xy} = 0 . \tag{21}$$

As can be seen, ε^0_x could only vary in the y direction and ε^0_y could only vary in the x direction. This was felt to be restrictive.

In the latest work, to allow more freedom to the spatial variation of strain, the following functional forms have been used to approximate for the inplane elongation strains,

$$\varepsilon_x^0 = \frac{\partial u^0}{\partial x} + \frac{1}{2}\left(\frac{\partial w}{\partial x}\right)^2 = a_1 + a_2x^2 + a_3y^2 + a_4x^2y^2 \qquad (22)$$

$$\varepsilon_y^0 = \frac{\partial v^0}{\partial y} + \frac{1}{2}\left(\frac{\partial w}{\partial y}\right)^2 = b_1 + b_2y^2 + b_3x^2 + b_4x^2y^2 \ . \qquad (23)$$

The a_i and b_i are to-be-determined constants. These functions are less restrictive than the previously approximate strain fields. In the present work the elongation strains are allowed to vary in both the x and y directions. Only even powers of x and y have been used in the approximate strain functions. This is because it has been assumed that in moving away from the central portion of the laminate (the origin in fig. 1a), the elongation strains increase, or decrease, as the edges of the laminate are approached, independent of which edge.

Using w(x,y) from eq. 1 in eqs. 22 and 23 and integrating eq. 22 with respect to x and eq. 23 with respect to y results in

$$u^0(x,y) = a_1x + \frac{a_2x^3}{3} + a_3xy^2 + \frac{a_4x^3y^2}{3} + g(y) - \frac{a^2x^3}{6} \qquad (24)$$

$$v^0(x,y) = b_1y + \frac{b_2y^3}{3} + b_3x^2y + \frac{b_4x^2y^3}{3} + h(x) - \frac{b^2y^3}{6} \ . \qquad (25)$$

In these results g(y) is an arbitrary function of y and h(x) is an arbitrary function of x. For cross-ply laminates, it is expected that $u^\circ(o,y) = 0$ and $v^\circ(x,0) = 0$. For this to be true it is required that

$$g(y) = h(x) = 0 \ . \qquad (26)$$

Substituting eqs. 24 and 25 into eq. 7 leads to

$$\varepsilon^0_{xy} = \frac{1}{2}\left\{2(a_3 + b_3)\, xy + \frac{2}{3}\,(a_4 x^3 y + b_4 x y^3) + abxy\right\} . \qquad (27)$$

If, as in the previous work, it is assumed that the inplane shearing strains are negligible when compared to the inplane elongation strains, then it is necessary that

$$2(a_3 + b_3) + ab = 0 , \qquad (28)$$

and

$$a_4 = 0 = b_4 , \qquad (29)$$

If it is assumed that

$$a_3 = b_3 = -\frac{ab}{4} , \qquad (30)$$

then, for the purposes of comparison, the present displacement field can be reduced to that of the previous study, eqs. 17 and 18, by setting a_2 and b_2 to zero. In addition, eq. 28 is also satisfied. Using eq. 30, the assumed inplane strain fields become

$$\varepsilon^0_x = a_1 + a_2 x^2 - \frac{aby^2}{4} \qquad (31)$$

$$\varepsilon^0_y = b_1 + b_2 y^2 - \frac{abx^2}{4} \qquad (32)$$

$$\varepsilon^0_{xy} = 0 \qquad (33)$$

In the latest formulation, then, the inplane elongation strains can vary with both the x and y coordinate. These approximate expressions for inplane strains are used in the expression for total potential energy of the laminate. The potential energy expression is then subject to minimization with respect to a, b, a_1, b_1, a_2, and b_2.

Minimization of Potential Energy

The total potential energy, W, for the laminate is [5]

$$W = \int_{Vol} \omega \, dVol, \tag{34}$$

where ω is the strain energy density and is given by

$$\omega = \frac{1}{2} c_{ijkl} e_{ij} e_{kl} - \beta_{ij} e_{ij} \Delta T . \tag{35}$$

The c_{ijkl} are the elastic constants of the material and the β_{ij} are constants related to the elastic constants and the coefficients of thermal expansion of the material. The temperature change, from curing to room temperature, is ΔT. Cooling corresponds to a negative ΔT. The e_{ij} are of course the strains. All material properties are assumed to be independent of temperature. This is not a restriction on the approach because temperature-dependent properties could be easily incorporated into the theory, since $\Delta T \neq \Delta T(x,y)$. With the form of eq. 35, the datum ($\omega = 0$) for the potential energy is the elevated cure temperature and the net work of any external tractions acting on the laminate as it cools and deforms to its final shape is assumed to be zero.

As is usually the case with laminate analysis, the z-direction stresses are assumed negligible and the elastic properties of the individual lamina are represented by the familiar reduced stiffnesses referred to the x-y system, $\bar{Q}_{ij}$. The β_{ij} can then be related to the $\bar{Q}_{ij}$'s and the lamina coefficients of thermal expansion in the x and y directions, α_x and α_y respectively. The expression for the strain energy density then becomes

$$\omega = \frac{1}{2}\left(\bar{Q}_{11}e_{11}^2 + \bar{Q}_{12}\,e_{11}e_{22} + 2\bar{Q}_{11}e_{12}^2 + \frac{1}{2}\,\bar{Q}_{22}e_{22}^2\right)$$

$$- \left(\bar{Q}_{11}\alpha_x + \bar{Q}_{12}\alpha_y\right) e_{11}\Delta T - \left(\bar{Q}_{12}\alpha_x + \bar{Q}_{22}\alpha_y\right) e_{22}\Delta T. \qquad (36)$$

Because these are cross-ply laminates, there is no α_{xy}. Using eqs. 1-4 and 31-33 in eq. 36, the expression for the total potential energy of the laminate is of the form

$$W = \int_{z=-\frac{h}{2}}^{\frac{h}{2}} \int_{y=-\frac{L_y}{2}}^{\frac{L_y}{2}} \int_{x=-\frac{L_x}{2}}^{\frac{L_x}{2}} \omega(a,\ b,\ a_1,\ b_1,\ a_2,\ b_2,\ \bar{Q}_{ij}\ \alpha_x,\ \alpha_y,\ \Delta T,\ x,\ y,\ z)\ dxdydz\ . \qquad (37)$$

With the limits on the integral, it is assumed that the laminate is of thickness h and has a length of L_x in the x direction and L_y in the y direction.

The integral of eq. 37, due to the multiplying and squaring of the strain expressions, is quite lengthy. However, the spatial integrations on these expressions are straightforward. Integration of the variables z and $\bar{Q}_{ij}$ leads to the familiar A, B and D matrices of classical lamination theory. Integration of the variables z, $\bar{Q}_{ij}$, α_x, α_y, and ΔT leads to effective inplane resultant forces and effective thermal moments. These are the same expressions as obtained in classical lamination theory. Integration with respect to variables x and y results in terms which render the problem nonlinear and which dictates how the size of the laminate affects its room-temperature shape. Ultimate interest is in the first variation of W with respect to the unknown variables a, b,

a_1, b_1, a_2, and b_2. The theorem of minimum total potential energy requires that

$$\delta W = \left(\frac{\partial W}{\partial a}\right) \delta a + \left(\frac{\partial W}{\partial b}\right) \delta b + \left(\frac{\partial W}{\partial a_1}\right) \delta a_1 + \left(\frac{\partial W}{\partial b_1}\right) \delta b_1 + \left(\frac{\partial W}{\partial a_2}\right) \delta a_2 + \left(\frac{\partial W}{\partial b_2}\right) \delta b_2 \equiv 0 \ . \tag{38}$$

The actual taking of the first variation results in an equation of the form,

$$\begin{aligned} \delta W = {} & f_1(a, b, a_1, b_1, a_2, b_2)\, \delta a + f_2(a, b, a_1, b_1, a_2, b_2)\, \delta b \\ & + f_3(a, b, a_1, b_1, a_2, b_2)\, \delta a_1 + f_4(a, b, a_1, b_1, a_2, b_2)\, \delta b_1 \\ & + f_5(a, b, a_1, b_1, a_2, b_2)\, \delta a_2 + f_6(a, b, a_1, b_1, a_2, b_2)\, \delta b_2 . \end{aligned} \tag{39}$$

The f_i are algebraic relations between the six unknown constants a, b, a_1, b_1, a_2, and b_2, the geometric and elastic properties of the laminate, and the temperature change ΔT. For $\delta W = 0$, the six f_i must all be zero. The values of a, b,...etc. which make all six f_i equal to zero describe the equilibrium shapes of the laminates. The functions f_i are written out explicitly in the appendix.

Solution Procedure and Stability Considerations

Close examination of the f_i shows that four of the six of the equations are linear in a_1, b_1, a_2, and b_2 (these are the first four f_i in the appendix). Using these four equations, a_1, b_1, a_2, and b_2 are solved for in terms of a and b and substituted into the remaining two equations. This results in two nonlinear equations in a and b. By specifying the geometric and material properties of a particular laminate, numerical values of a and b can be determined using a Newton-type scheme. The numerical values of a and b can then be back-substituted to obtain values for a_1, b_1, a_2, and b_2.

As with the earlier study, there are either three real solutions or one real solution to the set of equations. Each solution corresponds to a different room-temperature, or equilibrium, shape. To complete the solution process, each equilibrium solution has to be checked for stability. This is a standard procedure for any nonlinear analysis which involves multiple equilibrium configurations. The form of the problem here, eq. 39, is of the form discussed by Simitses [6]. For an equilibrium configuration to be stable, the following matrix has to be positive definite:

$$\begin{bmatrix} \frac{\partial f_1}{\partial a} & \frac{\partial f_1}{\partial b} & \frac{\partial f_1}{\partial a_1} & \frac{\partial f_1}{\partial b_1} & \frac{\partial f_1}{\partial a_2} & \frac{\partial f_1}{\partial b_2} \\ \frac{\partial f_2}{\partial a} & \frac{\partial f_2}{\partial b} & \frac{\partial f_2}{\partial a_1} & \frac{\partial f_2}{\partial b_1} & \frac{\partial f_2}{\partial a_2} & \frac{\partial f_2}{\partial b_2} \\ \frac{\partial f_3}{\partial a} & \frac{\partial f_3}{\partial b} & \frac{\partial f_3}{\partial a_1} & \frac{\partial f_3}{\partial b_1} & \frac{\partial f_3}{\partial a_2} & \frac{\partial f_3}{\partial b_2} \\ \frac{\partial f_4}{\partial a} & \frac{\partial f_4}{\partial b} & \frac{\partial f_4}{\partial a_1} & \frac{\partial f_4}{\partial b_1} & \frac{\partial f_4}{\partial a_2} & \frac{\partial f_4}{\partial b_2} \\ \frac{\partial f_5}{\partial a} & \frac{\partial f_5}{\partial b} & \frac{\partial f_5}{\partial a_1} & \frac{\partial f_5}{\partial b_1} & \frac{\partial f_5}{\partial a_2} & \frac{\partial f_5}{\partial b_2} \\ \frac{\partial f_6}{\partial a} & \frac{\partial f_6}{\partial b} & \frac{\partial f_6}{\partial a_1} & \frac{\partial f_6}{\partial b_1} & \frac{\partial f_6}{\partial a_2} & \frac{\partial f_6}{\partial b_2} \end{bmatrix} \quad (40)$$

Using the definitions of the f_i, explicit algebraic expressions are obtained for each term in the matrix. For each equilibrium solution, the numerical values of a, b, a_1, b_1, a_2, and b_2 are substituted into each term of the matrix and positive definiteness assessed. If the matrix is positive definite, the equilibrium configuration is stable.

Numerical Results

In what follows, all numerical results are based on laminates with the following material properties:

$$E_1 = 181 \text{ GPa } (26.2 \times 10^6 \text{ psi})$$

$$E_2 = 10.3 \text{ GPa } (1.49 \times 10^6 \text{ psi})$$

$$\nu_{12} = 0.28$$

$$G_{12} = 7.17 \text{ GPa } (1.04 \times 10^6 \text{ psi})$$

$$\alpha_1 = -0.106 \times 10\text{-}6/°C/ \ (-0.059 \times 10\text{-}6/°F)$$

$$\alpha_2 = 25.6 \times 10^{-6}/°C \ (14.2 \times 10^{-6}/°F) \ .$$

The sidelengths L_x and L_y are assumed to be equal (square laminates) so that $L_x = L_y = L$. The shapes are studied as a function of stacking sequence and sidelength. The sidelengths are in the range $0 \leq L \leq 800$ mm ($\simeq 32$ in).

Figure 3 shows the shape characteristics of square $[0_2/90_2]_T$ laminates as a function of sidelength. Note the break in the horizontal scale on this figure. The upper portion of fig. 3 shows the x-direction curvature, a, as a function of L the lower portion shows the y-direction curvature, b, as a function of L. Since these are cross-ply laminates, a and b are the principal curvatures. In the x-y coordinate system there is no twist curvature. Also note that the relation between b and L is identical to the relation between a and L except for sign. The solution characteristics have several branches. These branches are identified by the letters A, B, C, D, and E. It should be noted that as L increases, the curvature values of branch BD approach zero. In addition, for $L > 300$ mm ($\simeq 12$ in.) the curvature values for branch BE of the upper figure and branch BC of the lower figure are actually zero. In the figures these branches have been separated from the horizontal

axes to show their existence. The horizontal axes have been broken to show the details of the curvature characteristics for sidelengths less than 100 mm (≈ 4 in.). As a result, the distinction between branch BD and the zero-curvature branches becomes vague near the right end of the figures. However, the branches are distinct for all L. It should be pointed out that the solution corresponding to L = 0 is the classical lamination theory solution.

The shape characteristics shown in fig. 3 are virtually indistinguishable from the shape characteristics obtained using the more limited approximate displacement fields, eqs. 17 and 18. Thus, the more sophisticated inplane functional forms do not affect the predicted out-of-plane displacements to any significant degree.

The stability analysis shows branch AB represents a stable equilibrium solution. Since b = -a on this branch, the branch represents laminates which exhibit saddle shapes at room temperature. Branch BD, a continuation of the saddle branch, is shown to be unstable. Branch BC is stable and corresponds to laminates which have a large curvature in the x direction and a small curvature in the y direction. As the sidelength L increases, the y-direction curvature asymptotically approaches zero. This branch represents circular cylinders with generators in the y direction. Branch BE is also stable and, in the limit of large L, corresponds to laminates with large curvature in the y direction and no curvature in the x direction, i.e., cylinders with generators in the x direction. Thus, a square $[0_2/90_2]_T$ laminate with a sidelength less than 35 mm (≈ 1.4 in.) will cure to the saddle shape. Generally, for non-zero sidelength the saddle will be shallower than the saddle predicted by classical lamination theory. For laminates greater than 75

mm (≈ 3 in.) on a side, the room-temperature shape will be one of two cylindrical shapes. To get from one shape to the other requires a snap-through action. Laminates with sidelengths in the range 35-75 mm will have two possible shapes and a snap-through action is also required to get from one shape to another. Neither shape will have associated with it a direction of zero curvature. For either shape, one curvature will be much smaller than the other and as the laminate sidelength increases beyond 75 mm, the smaller curvature will asymptotically approach zero.

Although the effect of the more sophisticated inplane displacement fields on the predicted out-of-plane deformations is negligible, their effects on inplane strains could be important. Surprisingly, the effect is also negligible. Figure 4 shows the predicted inplane residual strains, ε_x^0 and ε_y^0, as a function of spatial location for two $[0_2/90_2]_T$ laminates. One laminate has a sidelength of 150 mm (≈ 6 in.) while the other laminate has a sidelength of 800 mm (≈ 32 in.). Based on the results of fig. 3, both laminates are cylindrical. For the cases shown, the cylinders have generators in the y direction (fig. 1c and branch BC of fig. 3). The strains were computed using eqs. 31 and 32, functional forms which allow spatial variations of strain in both the x and y direction. As can be seen, for the larger cylinder both inplane elongation strains are spatially invariant. For the smaller laminate, ε_x^0 varies slightly in the y direction and is independent of x. On the other hand, for the smaller laminate, ε_y^0 varies slightly with x but is independent of y. Examination of eqs. 19 and 20, the strains assumed in the previous theory, shows that neither the x variation of ε_x^0 nor the y variation of ε_y^0 was allowed. This apparently was not as restrictive as first felt since, from fig. 4, there is no tendency of ε_x^0 to vary with x

or ε_y^0 to vary with y. In fact, the strains predicted using the previous theory are indistinguishable from the strains predicted by the present theory. As a matter of interest, classical lamination theory predicts ε_x^0 and ε_y^0 to be -905×10^{-6} for these cases. The elongation strains associated with the direction of nonzero curvature are very close to the predictions of classical lamination theory. The strains associated with the direction of zero curvature are lower. As will be pointed out later, the curvature of the cylinder is also roughly the value of one curvature of the saddle predicted by the classical theory. This can be seen by noting in the upper portion of fig. 3 that branch AC asymptotes close to the value given by point A ($L = 0$), the classical theory curvature prediction. The roles of ε_x^0 and ε_y^0 are reversed for the other cylindrical configurations at these lengths, i.e. $a = 0$ $b < 0$.

From the results of fig. 4, and from other strain studies not shown here, it appears that the larger the cylindrical laminate, the more spatially uniform the inplane strains become. It is important to note that the inplane strains are everywhere compressive. The laminate not only has a useful shape, a cylinder, but it is prestrained in compression. This compressive prestrain would be very useful if the cylinder were used, for example, as an internally pressurized vessel. Owing to the curvature, the strains away from the midsurface vary with through-the-thickness location. However, for the cases in fig. 4, all points in the laminates are in a state of compressive residual strain. The largest compressive strains occur in the matrix direction at the inner surface of the cylinder. The smallest compressive strains occur in the fiber direction at the outer surface. For thicker laminates, a $[0_4/90_4]_T$ for example, the thickness and curvature effects combine to produce tensile strains in the fibers at the outer surface.

Figures 5-7 show the shape characteristics of the other unsymmetric cross-ply laminates studied. All laminates are also square with the curvature characteristics in the x and y direction being illustrated as a function of sidelength. There is also a break in the horizontal scale of fig. 5. The horizontal scales of figs. 6 and 7 are continuous but the vertical scales of branch DBC in each figure have been exaggerated. For all laminates a and b are the principal curvatures. Stability considerations shows branch BD to be unstable for all laminates.

The $[0/90/0/90]_T$ shape characteristics are similar to the shape characteristics of the $[0/0/90/90]_T$. However, the shape characteristics of the $[0/0/0/90]_T$ and the $[0/0/90/0]_T$ are quite different. The most striking difference is the lack of a coalescence of the solution branches. This coalescence of solutions, which is denoted as point B in figs. 3 and 5, is often referred to as a bifurcation point. The disjoint behavior of the solution branches for the $[0/0/0/90]_T$ and $[0/0/90/0]_T$ is often referred to a limit point behavior. Generally, the existence of a bifurcation point, as opposed to the existence of a limit point, is associated with the analysis of a perfect or ideal case. In the problems here, the perfect cases are associated with 'perfect unsymmetry' or 'antisymmetry.' The $[0/0/90/90]_T$ and $[0/90/0/90]_T$ are antisymmetric. In contrast a $[1/0/90/90]_T$, for example, would exhibit limit point behavior rather bifurcation. The perfect asymmetry, or the lack of it, is reflected in the A, B, D matrices. Whereas as $[0/0/90/90]_T$ laminates cease to have a unique stable saddle shape when the sidelength exceeds 35 mm, $[0/90/0/90]_T$ laminates retain a unique saddle shape up to sidelengths of about 90 mm (≈ 3.5 in.). This is a reflection of the fact that the $[0/0/90/90]_T$ configuration has a greater, or more serious,

asymmetry than does the $[0/90/0/90]_T$ lay-up. The level of asymmetry is reflected in the B matrix. For sidelengths greater than 200 mm ≈ 8 in.) branches BC and BE of fig. 5 represent, respectively, cylinders with generators in the y and x directions. To get from one cylindrical shape to another requires a snap-through action. Like the $[0/0/90/90]_T$ cases, the relation between b and L is identical to the relation between a and L except for sign.

The $[0/0/0/90]_T$ and the $[0/0/90/0]_T$ are quite interesting and deserve some discussion. Of course, at zero sidelength the classical lamination theory saddle shape is predicted. Unlike the previous two cases, the curvatures of the saddle are not equal. As sidelength increases, the smaller of the two curvatures, a, is quickly suppressed to zero. The larger curvature, b, essentially remains unaffected by the sidelength dimension. For sidelengths between 100 and 180 mm, (≈ 4 and ≈ 7 in.), $[0/0/0/90]_T$ laminates cure to a cylindrical shape. What is is important is that this cylindrical shape is the only shape that can exist at those sidelengths. The cylindrical shape is unique and it is stable. For the 'perfect' cases, i.e. the $[0/0/90/90]_T$ and $[0/90/0/90]_T$, at sidelengths for which the cylindrical behavior appears, one cylinder can be snapped into another cylinder. For these cases the cylindrical shape appears only in the presence of another possible cylindrical shape and is thus a bistable configuration. From the results of fig. 6 it appears there is the potential for generating unique cylindrical shapes with unsymmetric laminates. Similar comments can be made concerning the uniqueness of shapes of $[0/0/90/0]_T$ laminates with sidelengths between 120 and 525 mm (≈ 5 and ≈ 21 in.).

For sidelengths greater than the length associated with point B, both the $[0/0/0/90]_T$ and the $[0/0/90/0]_T$ laminates exhibit two possible cylindrical shapes. The two cylindrical shapes possible with each laminate have curvatures of opposite sign and unequal magnitude. These cylindrical shapes are bistable. It is not clear, however, that the amount of force required to make the snap from BC to AE is the same as the force required to make the reverse snap. The equality of snap-through force is most likely the case for the $[0/0/90/90]_T$ and $[0/90/0/90]_T$ laminates.

There are some interesting similarities among the four laminates considered. In all cases all branches are stable except branch BD. In each case BD represents all or part of a saddle-shaped configuration. It appears, then, the shape qualitatively predicted by classical lamination theory is often inherently an unstable configuration. Also for all cases, as laminate sidelength increases slightly from zero, say up to 30 mm (1.2 in.), the curvatures seem to decrease. For $[0/0/0/90]_T$ and $[0/0/90/0]_T$ laminates, the smaller of the two curvatures, the x-direction curvature, decreases rapidly toward zero. The major curvature, the y-direction curvature, decreases slightly. In the earlier experimental studies [1] this suppression of the smaller curvature was observed to always be the case. For $[0/0/90/90]_T$ and $[0/90/0/90]_T$ laminates, as sidelength increases slightly from zero, both the x and y curvatures decrease considerably but they do not go to zero. In all cases, as sidelengths increase beyond 30 mm, if one of the curvatures is not zero, it eventually becomes zero. The other curvature eventually returns to a value close to the value predicted by classical lamination theory. Specifically, for both the $[0/0/90/90]_T$ and $[0/90/0/90]_T$ laminates, the y-

direction curvature decreases, in magnitude, and then increases along path ABE, as in the lower portion of fig. 3. The x-direction curvature decreases and is ultimately suppressed to zero along path ABE, as in the upper portion of fig. 3. For both the $[0/0/0/90]_T$ and the $[0/0/90/0]_T$ laminates, the y-direction or major curvature decreases slightly in magnitude and then increases along path AE, as in the lower portion of fig. 6. The x-direction or minor curvature is suppressed to zero along AE, as in the upper portion of fig 6. For the perfectly asymmetric cases, path ABC exhibits similar decreasing-suppression and decreasing-increasing curvature behavior for the two curvatures involved.

Though not shown, the residual strain levels for all four laminates are similar. There is nothing unusual about the spatial variation of strain for any of the laminates considered. Although the magnitudes of the strains are different among the four laminates studied, fig. 3 is representative of the strain behavior for all cylindrical configurations of all laminates.

Acknowledgements

The work reported on here was conducted while the author was being supported by NASA Cooperative Agreement NCCI-15 and AFOSR Grant 81-0195. The financial support of the two funding agencies is gratefully acknowledged.

References

1. Hyer, M. W., "Some Observations on the Room-Temperature Shapes of Unsymmetrically Laminated Composites," J. Comp. Materials, Vol. 15, pp. 175-194, 1981.

2. Hyer, M. W., "Calculation of the Room-Temperature Shapes of Unsymmetrically Laminated Composites," J. Comp. Materials, Vol. 15, pp. 296-311, 1981.

3. Hahn, H. T., "Warping of Unsymmetric Cross-Ply Graphite/Epoxy Laminates," Composites Technology Review, Vol. 3, No. 3, pp. 114-117, 1981.

4. Hahn, H. T. and Hwang, D. G., "Residual Stresses and Their Effects in Composite Laminates," Proceeding of Symposium on Engineering Science and Mechanics, Tainan, Taiwan, Dec. 1981.

5. Fung, Y. C. Foundations of Solid Mechanics, Prentice-Hall, Inc., Englewood Cliffs, NJ, 1965, p. 354.

6. Simitses, G. J. An Introduction to the Elastic Stability of Structures, Prentice-Hall, Inc. Englewood Cliffs, NJ, 1976, pp. 8-14.

APPENDIX

GOVERNING ALGEBRAIC EQUATIONS

The following six equations govern the equilibrium shapes of the laminate.

$$f_1 = A_{11}a_1 + G_9a_2 + A_{12}b_1 + 4C_6b_2 - N_x^T - C_1ab - B_{11}a - C_4ab \quad \text{A-1}$$

$$f_2 = A_{12}a_1 + 4C_4a_2 + A_{22}b_1 + G_{10}b_2 - N_y^T - C_6ab - C_7ab - B_{22}b \quad \text{A-2}$$

$$f_3 = G_9a_1 + G_{14}a_2 + 4C_4b_1 + \frac{2304}{144}C_5b_2 - N_x^T\frac{L_x^2}{2} - G_1ab - G_2a - G_6ab \quad \text{A-3}$$

$$f_4 = 4C_6a_1 + \frac{2304}{144}C_5a_2 + G_{10}b_1 + G_{15}b_2 - N_y^T\frac{L_y^2}{2} - G_3ab - G_7ab - G_8b \quad \text{A-4}$$

$$f_5 = - C_1a_1b - G_1a_2b + C_2ab^2 + C_3ab - B_{11}a_1 - G_2a_2 + C_3ab + D_{11}a - C_6b_1b - G_3b_2b + C_5ab^2 + D_{12}b - C_4a_1b - G_6a_2b + C_5ab^2 - G_7b_1b - G_7b_2b + C_8ab^2 + C_9b^2 + (N_x^T\frac{L_y^2}{48})b + (N_y^T\frac{L_x^2}{48})b + M_x^T \quad \text{A-5}$$

$$f_6 = - C_1 a_1 a - G_1 a_2 a + C_2 a^2 b + C_3 a^2 - C_6 a b_1$$
$$- G_3 a b_2 + C_5 a^2 b - C_4 a_1 a - G_6 a_2 a + C_{15} a^2 b$$
$$+ D_{12} a - C_7 b_1 a - G_7 b_2 a + C_8 a^2 b + C_9 a b$$
$$- B_{22} b_1 - G_8 b_2 + C_9 a b + D_{22} b + (N_x^T - \frac{L_y^2}{48}) a$$
$$+ (N_y^T \frac{L_x^2}{48}) a + M_y^T \quad . \qquad \text{A-6}$$

The constants in the equations are defined by:

$C_1 = A_{11} L_y^2/48$ $\qquad$ $G_1 = A_{11} L_x^2 L_y^2/576$

$C_2 = A_{11} L_y^4/1280$ $\qquad$ $G_2 = B_{11} L_x^2/12$

$C_3 = B_{11} L_y^2/48$ $\qquad$ $G_3 = A_{12} L_y^4/320$

$C_4 = A_{12} L_x^2/48$ $\qquad$ $G_6 = A_{12} L_x^4/328$

$C_5 = A_{12} L_x^2 L_y^2/2304$ $\qquad$ $G_7 = A_{22} L_x^2 L_y^2/576$

$C_6 = A_{12} L_y^2/48$ $\qquad$ $G_8 = B_{22} L_y^2/12$

$C_7 = A_{22} L_x^2/48$ $\qquad$ $G_9 = A_{11} L_x^2/12$

$C_8 = A_{22} L_x^4/1280$ $\qquad$ $G_{10} = A_{22} L_y^2/12$

$C_9 = B_{22} L_x^2/48$ $\qquad$ $G_{14} = A_{11} L_x^4/80$

$G_{15} = A_{22} L_y^4/80$

The constants A_{11}, A_{12}, A_{22}, B_{11}, B_{22}, D_{11}, D_{22}, and D_{12} have their usual meaning. The N_x^T, N_y^T, M_x^T, and M_y^T are effective inplane thermal forces and moments, respectively, and are given by:

$$N_x^T = \Delta T \int_{-h/2}^{h/2} (\bar{Q}_{11}\alpha_x + \bar{Q}_{12}\alpha_y)dz; \quad N_y = \Delta T \int_{-h/2}^{h/2} (\bar{Q}_{12}\alpha_x + \bar{Q}_{22}\alpha_y)dz$$

$$M_x^T = \Delta T \int_{-h/2}^{h/2} (\bar{Q}_{11}\alpha_x = \bar{Q}_{12}\alpha_y)zdz; \quad M_y^T = \Delta T \int_{-h/2}^{h/2} (\bar{Q}_{12}\alpha_x + \bar{Q}_{22}\alpha_y)zdz$$

Fig. 1. Laminate shapes: (a) at the elevated curing temperature, and at room temperature, (b) a saddle shape, (c) a cylindrical shape, and (d) another cylindrical shape.

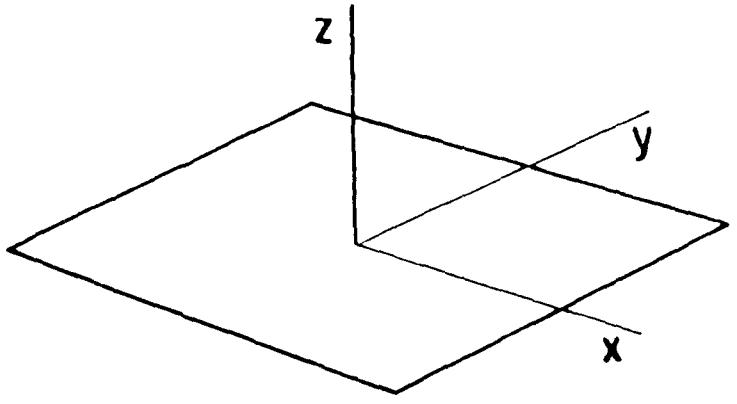

(a)

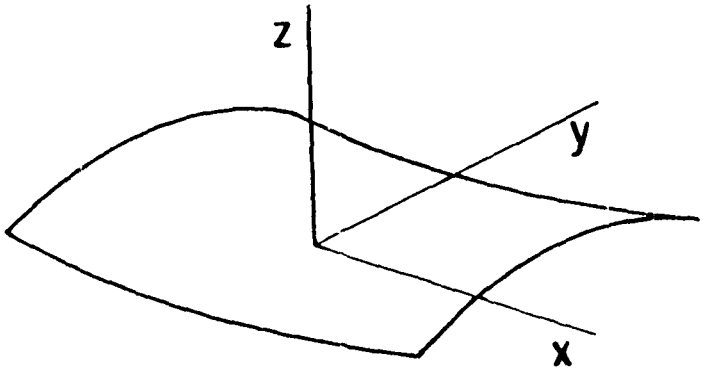

(b)

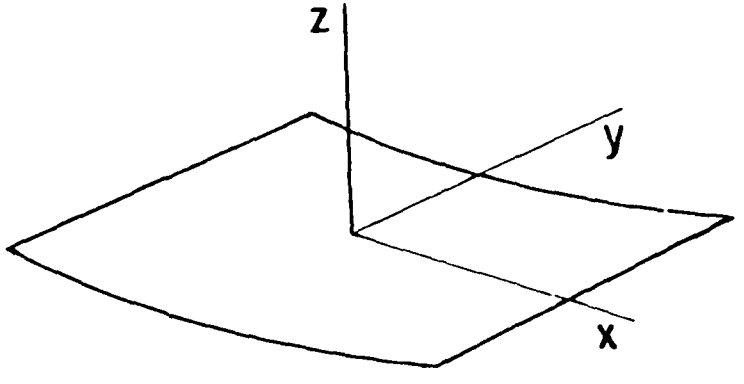

(c)

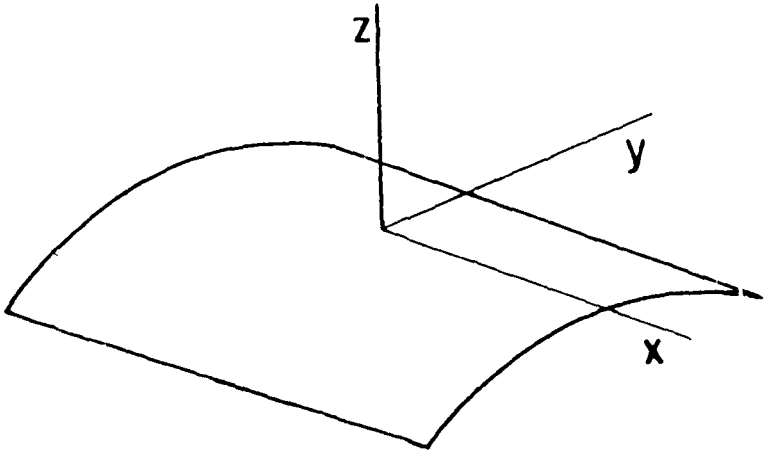

(d)

Fig. 2. Kinematics of a flat laminate deforming into a cylinder.

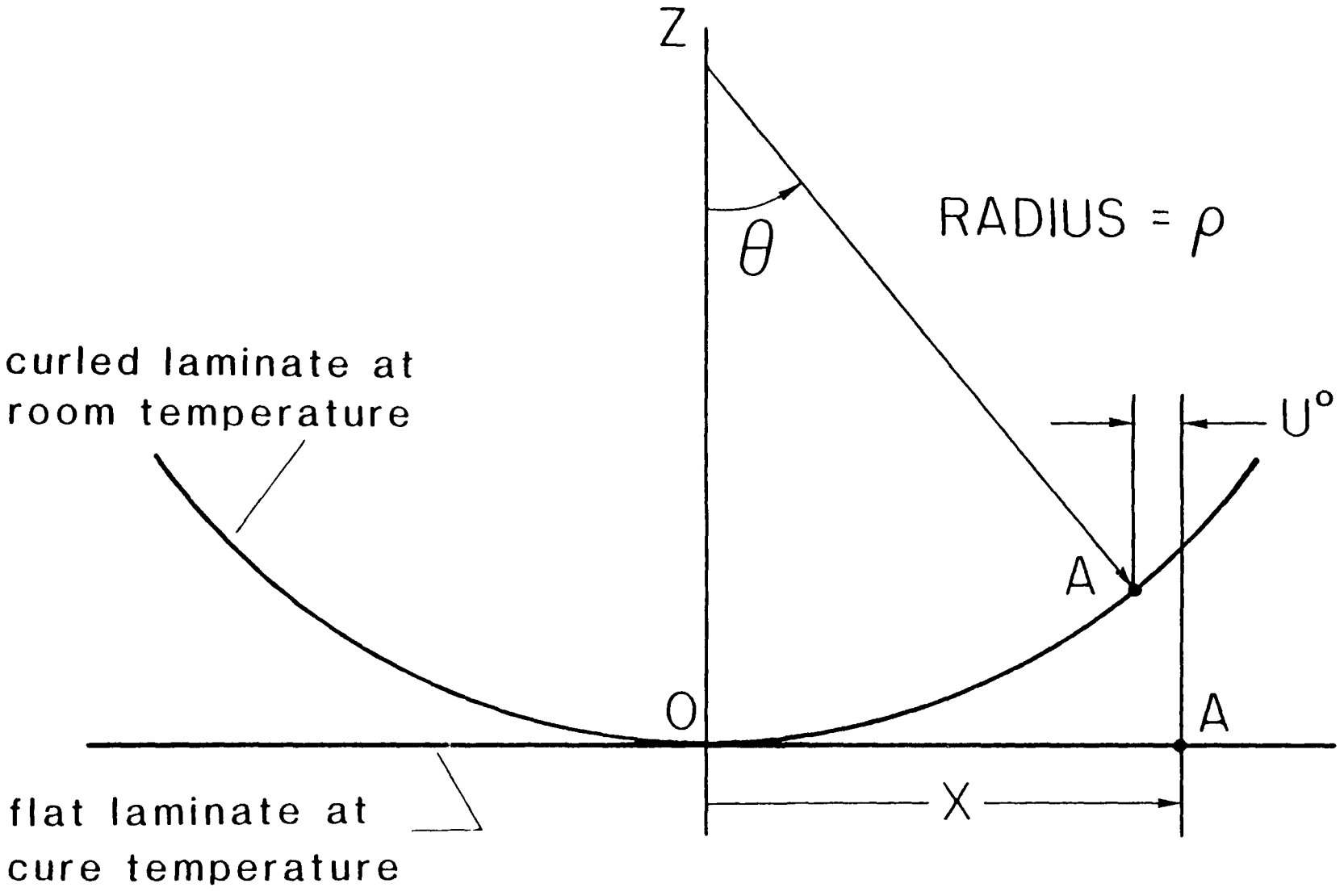
Z
θ
RADIUS = ρ
curled laminate at
room temperature
U°
A
O
A
X
flat laminate at
cure temperature

Fig. 3. Room-temperature shapes of square $[0/0/90/90]_T$ laminates.

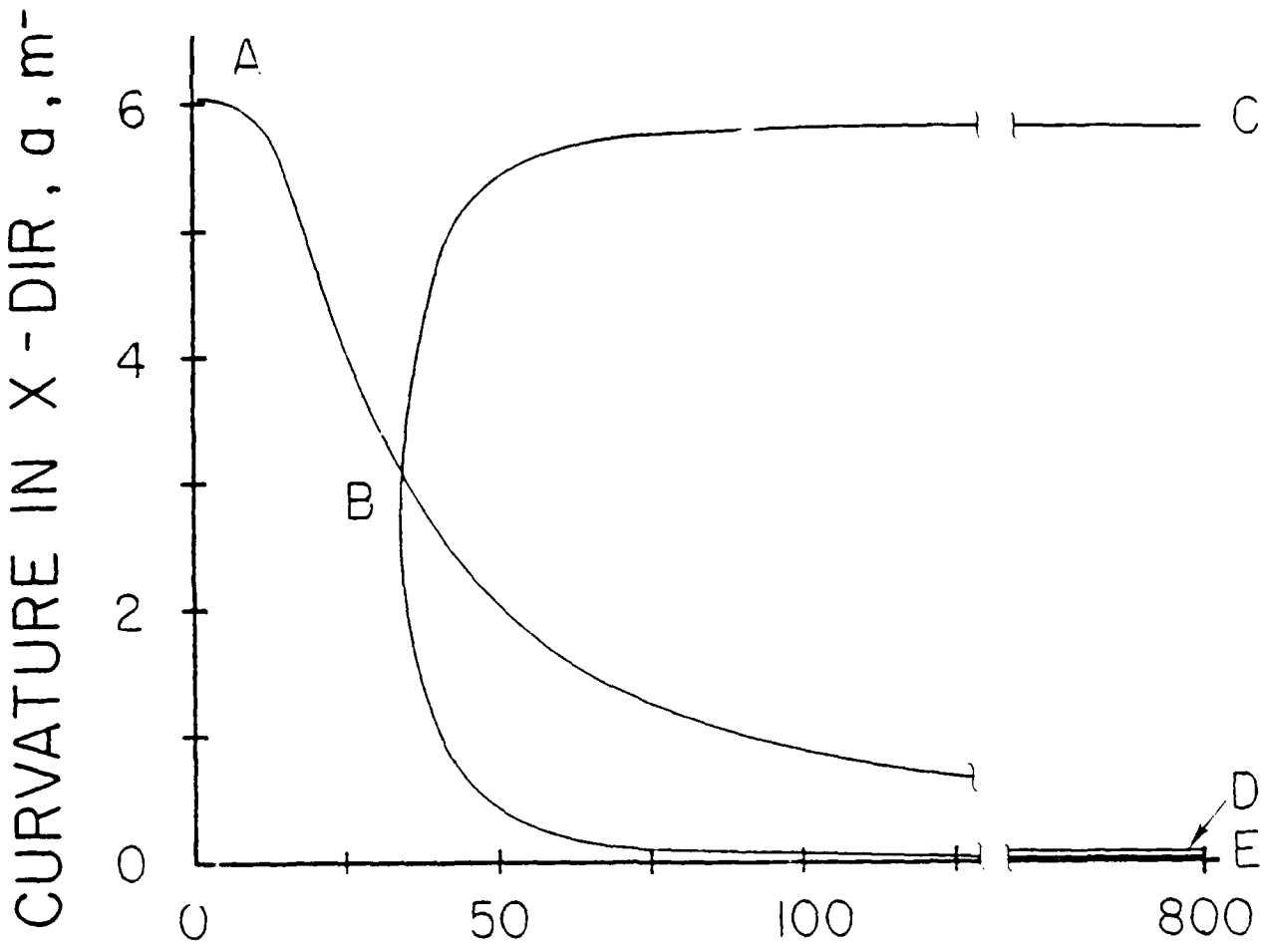
CURVATURE IN X-DIR., a, m⁻¹
6
4
2
0
A
B
C
D
E
0
50
100
800
LENGTH OF SIDE , L , mm

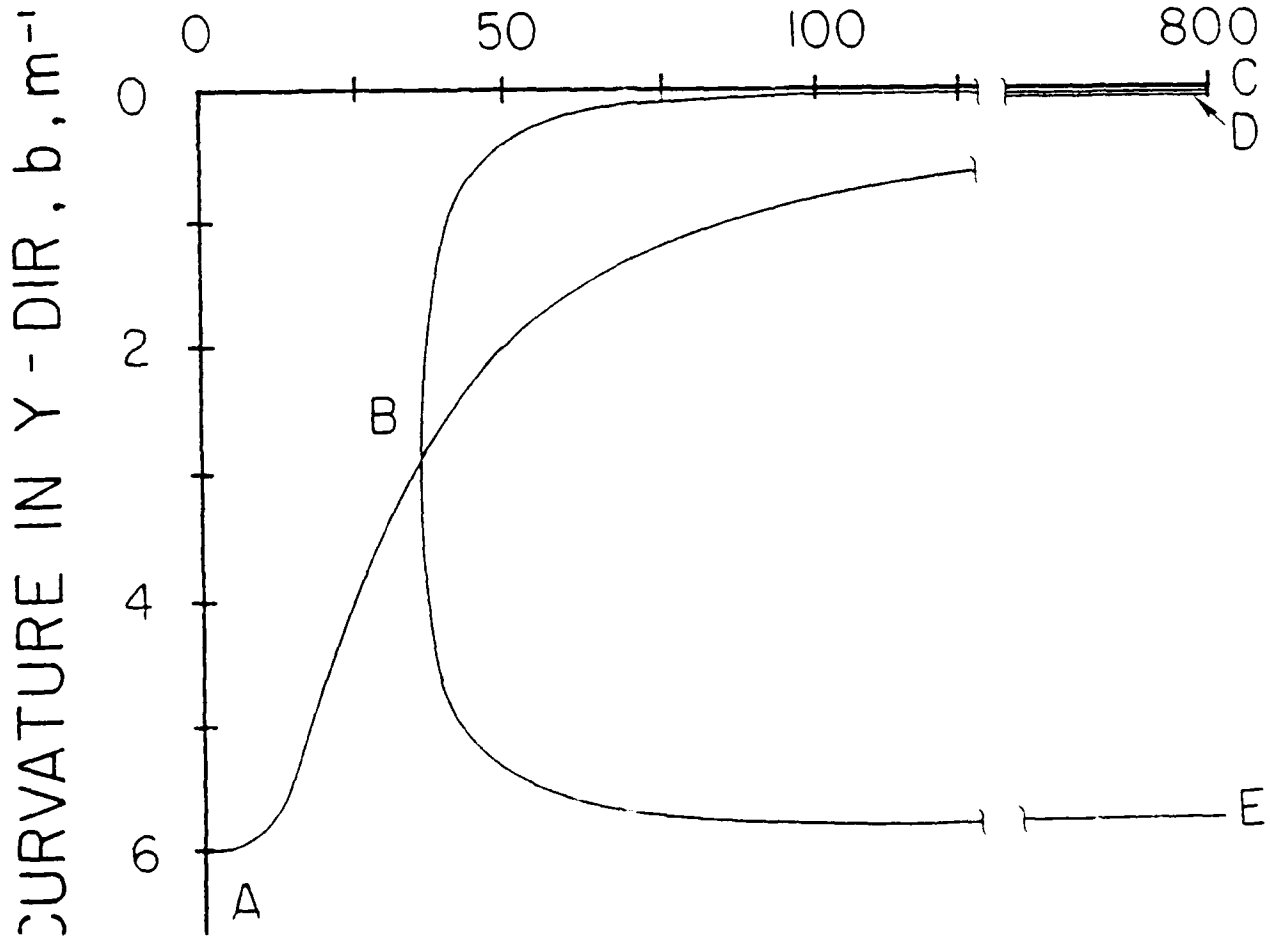
CURVATURE IN Y-DIR., b, m⁻¹
0
2
4
6
A
B
C
D
E
0
50
100
800

Fig. 4. Spatial dependence of residual inplane strains ε_x^0 and ε_y^0 for two $[0_2/90_2]_T$ cylindrical laminates.

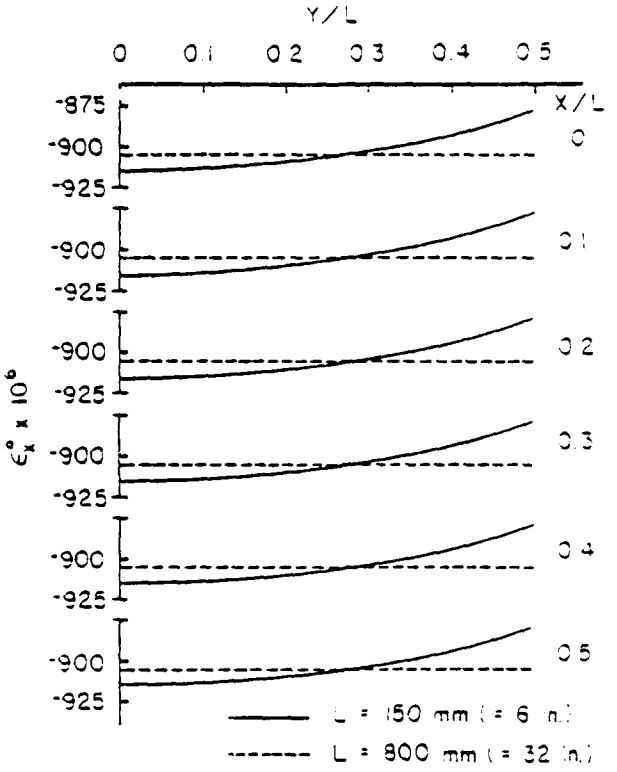
Y/L
0
0.1
0.2
0.3
0.4
0.5
X/L
-875
-900
-925
$\epsilon_x^o \times 10^6$
L = 150 mm (= 6 in.)
L = 800 mm (= 32 in.)

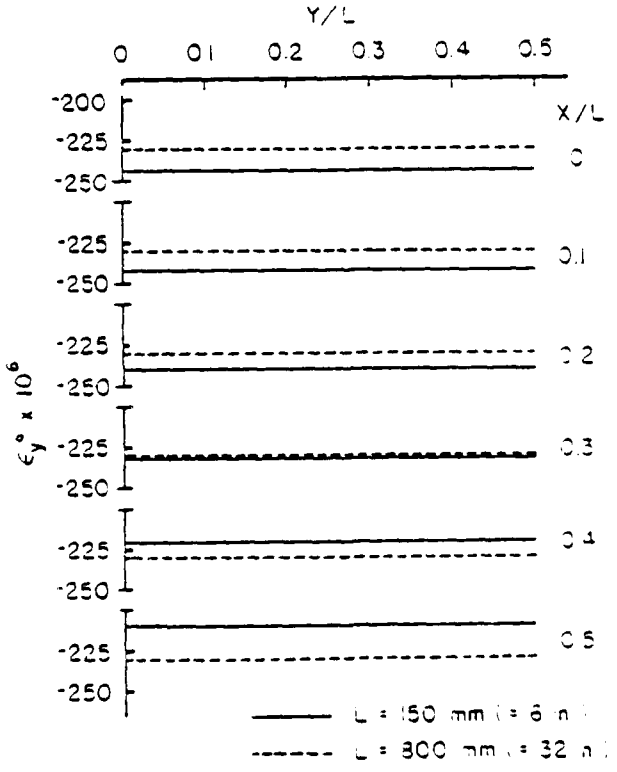
Y/L
0
0.1
0.2
0.3
0.4
0.5
X/L
-200
-225
-250
$\epsilon_y^o \times 10^6$
L = 150 mm (= 6 in.)
L = 800 mm (= 32 in.)

Fig. 5. Room-temperature shapes of square $[0/90/0/90]_T$ laminates.

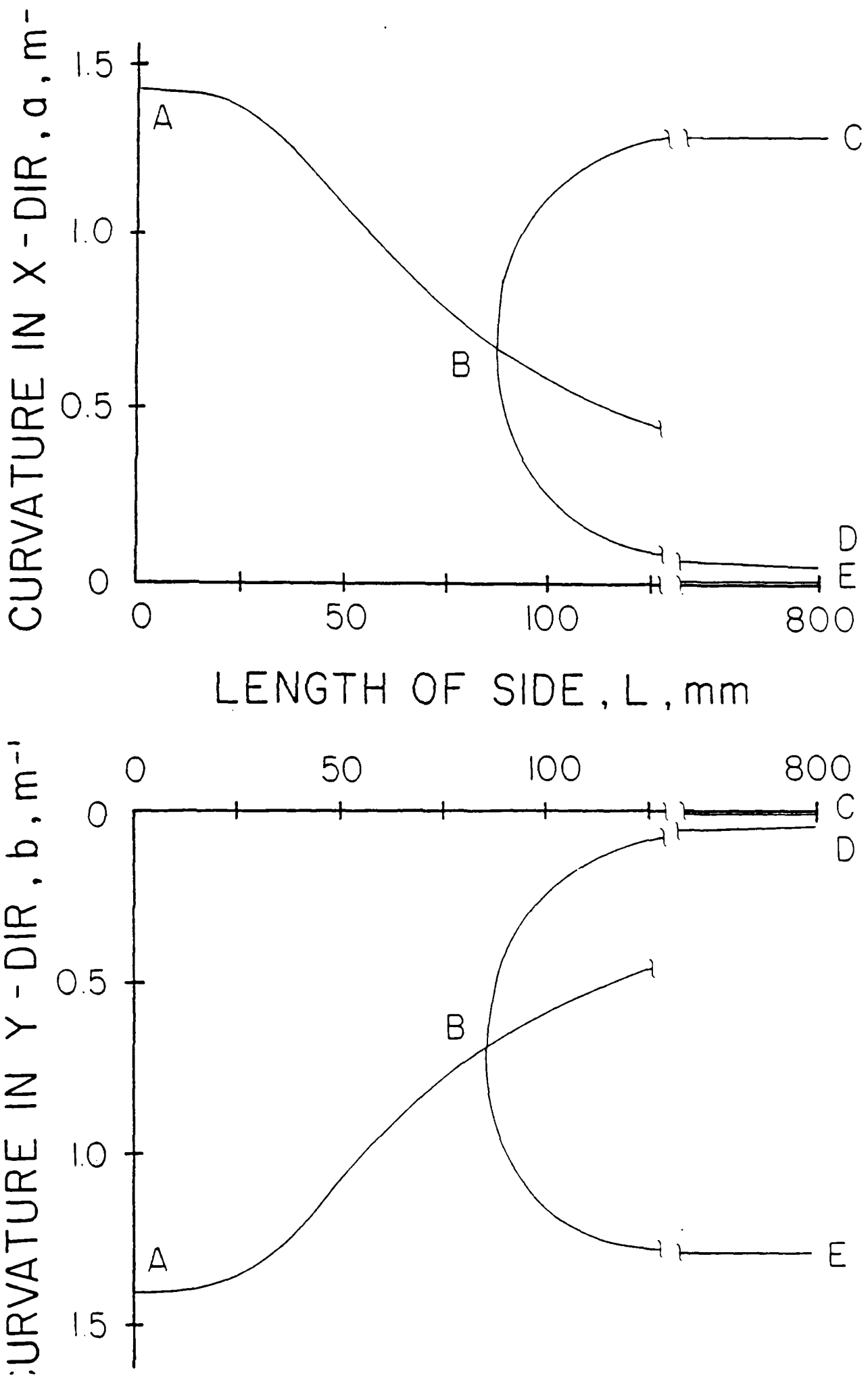
CURVATURE IN X-DIR., a, m-
1.5
1.0
0.5
0
A
B
C
D
E
0
50
100
800
LENGTH OF SIDE, L, mm
:URVATURE IN Y-DIR., b, m⁻¹
0
50
100
800
0
0.5
1.0
1.5
A
B
C
D
E

Fig. 6. Room-temperature shapes of square $[0/0/0/90]_T$ laminates.

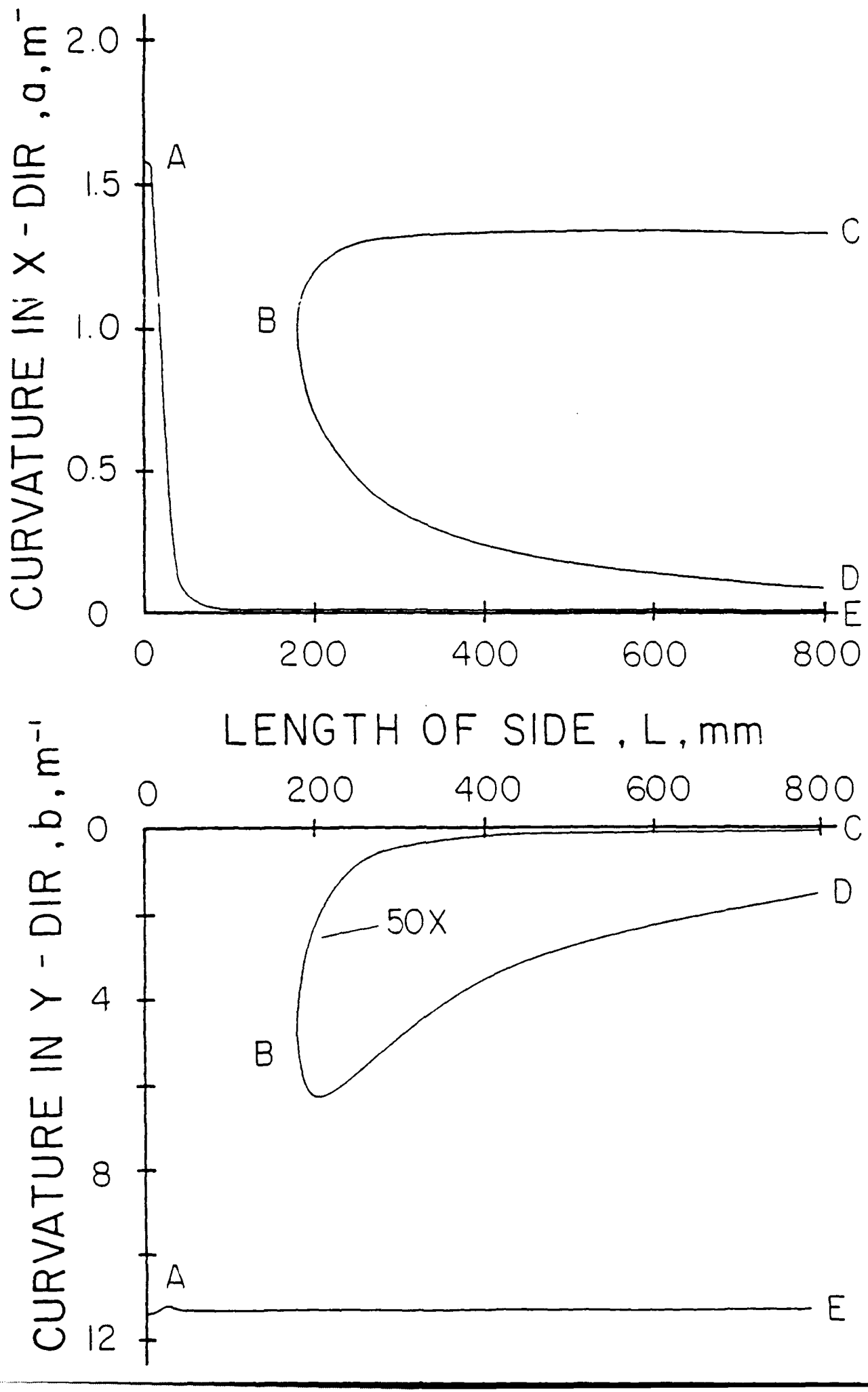
CURVATURE IN X - DIR , a , m⁻¹
2.0
1.5
1.0
0.5
0
A
B
C
D
E
0
200
400
600
800
LENGTH OF SIDE , L , mm
CURVATURE IN Y - DIR , b , m⁻¹
0
4
8
12
50X

Fig. 7. Room temperature shapes of square $[0/0/90/0]_T$ laminates.

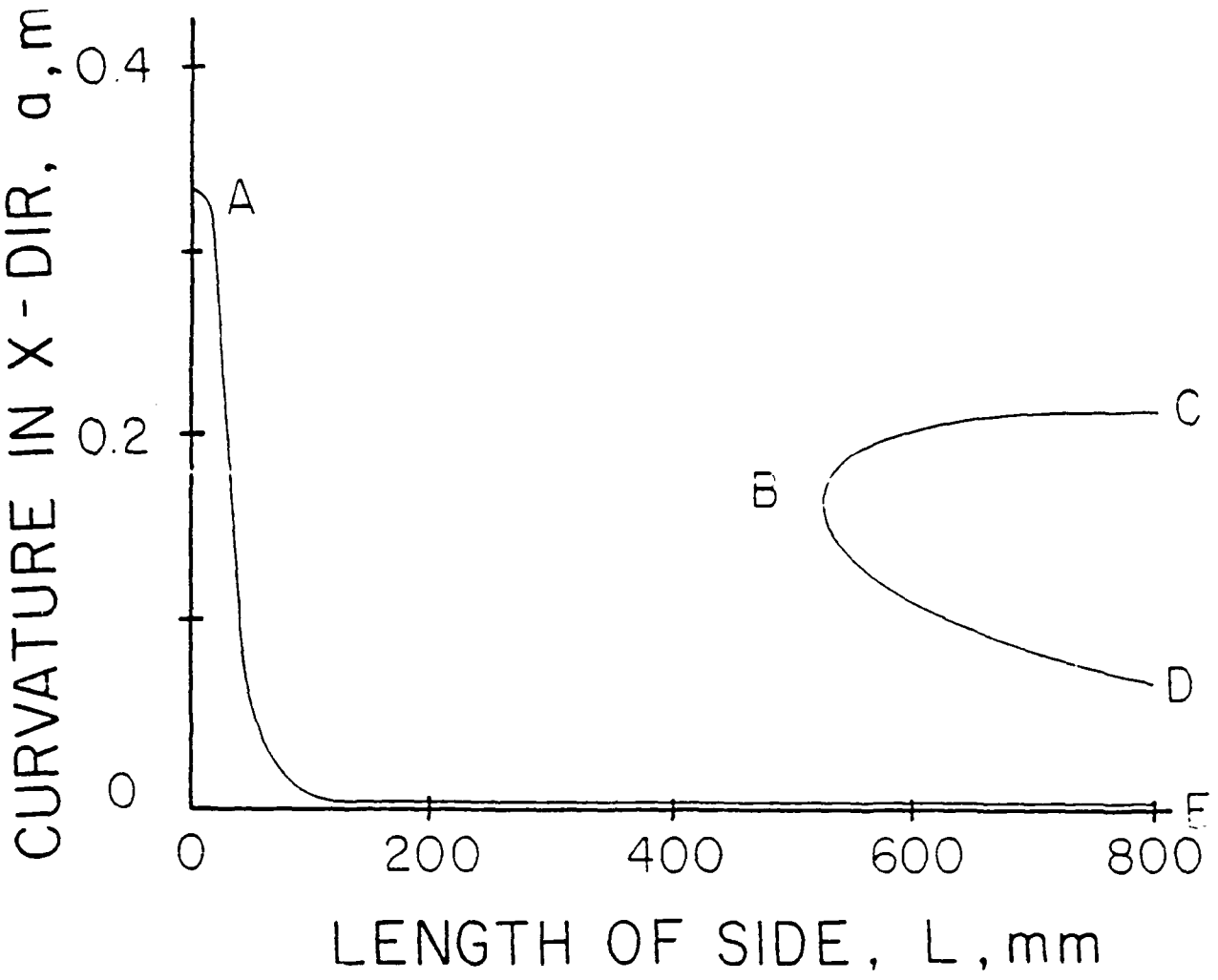
CURVATURE IN X-DIR, a, m
0.4
0.2
0
A
B
C
D
E
0
200
400
600
800
LENGTH OF SIDE, L, mm

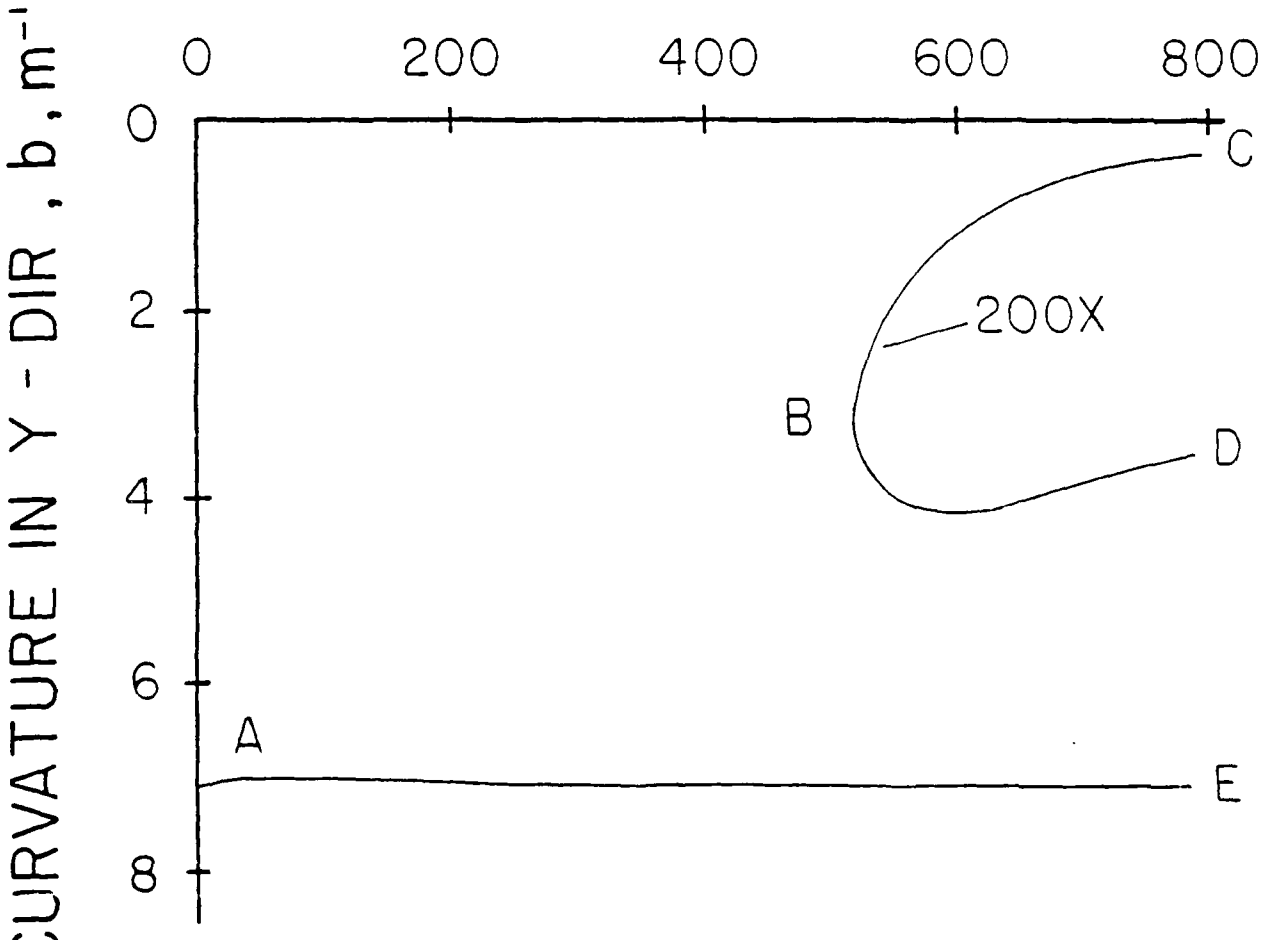
CURVATURE IN Y-DIR, b, m⁻¹
0
2
4
6
8
0
200
400
600
800
A
B
C
D
E
200X